Wavelet Families of Increasing Order in Arbitrary Dimensions

Jelena Kovačević, *Senior Member, IEEE,* and Wim Sweldens, *Member, IEEE*

Abstract—We build discrete-time compactly supported biorthogonal wavelets and perfect reconstruction filter banks for any lattice in any dimension with any number of primal and dual vanishing moments. The associated scaling functions are interpolating. Our construction relies on the lifting scheme and inherits all of its advantages: fast transform, in-place calculation, and integer-to-integer transforms. We show that two lifting steps suffice: predict and update. The predict step can be built using multivariate polynomial interpolation, while update is a multiple of the adjoint of predict. While we concentrate on the discrete-time case, some discussion of convergence and stability issues together with examples is given.

Index Terms—Interpolation, multivariate filter banks, wavelets.

I. INTRODUCTION

OVER the last decade, several constructions of compactly supported wavelets have originated both from signal processing and mathematical analysis. In signal processing, critically sampled wavelet transforms are known as filter banks or subband transforms [34], [44], [55], [57]. In mathematical analysis, wavelets are defined as translates and dilates of one fixed function and are used to analyze and represent general functions [23], [33]. Multiresolution analysis provided the connection between filter banks and wavelets [30], [33]. This lead to the construction of smooth, orthogonal and compactly supported wavelets [13]. The generalization to biorthogonality allowed the construction of symmetric wavelets and thus linear phase filters [8], [58]. For background material and more references on filter banks and wavelets, we refer the reader to [14], [47], and [59].

An obvious way to build wavelets in higher dimension is through tensor products of one-dimensional (1-D) constructions resulting in separable filters. However, this approach gives preferential treatment to the coordinate axes and only allows for rectangular divisions of the frequency spectrum. Often, symmetry axes and certain nonrectangular divisions of the frequency spectrum correspond better to the human visual system.

In the early 1990's, several solutions, both orthogonal and biorthogonal, and using different lattices became available [7], [10], [28], [36], [45]. These are typically concerned with two and three dimensions as the algebraic conditions in higher dimensions become increasingly cumbersome.

Other work in the signal processing literature uses two techniques: either cascade structures or one-to-multidimensional transformations. Although using cascade structures it is easy to build orthogonal or biorthogonal multidimensional filter banks [27], [28], one cannot guarantee vanishing moments which are a necessary condition for both stability and smoothness. One-to-multidimensional transformations include the method of separable polyphase components which cannot achieve perfect reconstruction for compactly supported filters [1], [4] as well as the McClellan transformation [20], [32]. The latter one preserves perfect reconstruction as well as zeros at aliasing frequencies and works only for zero-phase filters [4], [28], [26], [51].

In the approximation theory literature, one can also find many constructions of multidimensional wavelets. These constructions often use box splines on product lattices as scaling functions and again focus mostly on low dimensions [6], [16], [39]. In [37], the Quillin-Suslin theorem is used to build compactly supported box spline wavelets on separable lattices in $\mathbf{R}^s$. Recently, the lifting technique emerged providing a new angle for studying wavelet constructions [48], [49]. The original motivation behind lifting was to build time-varying perfect reconstruction filter banks, or second-generation wavelets. Even in the time-invariant setting, lifting offers several advantages and connects to many earlier approaches. The basic idea behind lifting is a simple relationship between all filter banks that share the same lowpass or the same highpass filter, also observed by Vetterli and Herley in [58]. Lifting also leads to a filter bank implementation known as ladder structures [2]. Moreover, it is known that all 1-D FIR filter banks fit into lifting [15], [31], [43], [53].

In this paper, we aim to provide a general recipe based on lifting for building filter banks and wavelets in *any* dimension, for *any* lattice and *any* number of primal and dual vanishing moments. To our knowledge, no such systematic construction exists. Our main result is a generalization of [48, Th. 12] which describes a 1-D family of biorthogonal wavelets associated to the interpolating Deslauriers-Dubuc scaling functions. This construction involves only two lifting steps, predict and update, where update is the adjoint of the predict divided by 2. We show that the same result holds in higher dimensions and for M channels as long as the update is chosen as the adjoint of the predict divided by M. The predict filter belongs to a class of filters we call Neville filters, which can be constructed using the de Boor-Ron algorithm for multidimensional polynomial interpolation [17], [18].

Our construction inherits all the built-in advantages of lifting such as custom design, in-place computation, integer-to-integer

transforms, and speed, the last one being particularly important in multiple dimensions. We show that the speed-up due to lifting is a factor M on the synthesis side, while it is at most two on the analysis side. As our construction results in interpolating scaling functions and halfband filters, it connects naturally to multidimensional interpolating subdivision [21], [38]. Our techniques allow the construction of a wavelet basis associated with any interpolating scaling function. Also, all wavelets built from interpolating scaling functions fit into our predict/update lifting framework.

This paper is organized as follows. Section I contains background material including an overview of multiresolution analysis in the multivariate case. Section II introduces Neville filters and shows how to build them. We then present our main result in two stages. Sections III deals with the two-channel case and contains several examples. The two-channel case sets the stage for the construction in the M-channel setting, presented in Section IV again including several examples. Finally, Section V discusses the fast transform algorithm.

II. NOTATION AND BACKGROUND MATERIAL

A. Signals and Operators

A signal x is a sequence of real-valued numbers indexed by the index set $\mathcal{K}$

$$x = \{x_k \in \mathbf{R} | k \in \mathcal{K}\} \in \mathbf{R}^{\mathcal{K}}$$

where $\mathcal{K}$ can be either a finite or an infinite set. In this paper, we focus on signals defined on a lattice in d-dimensional Euclidean space and thus always take $\mathcal{K} = \mathbf{Z}^d$. We say that a sequence is finite if only a finite number of x_k are nonzero.

For two sequences x and y of $\ell^2 = \ell^2(\mathcal{K})$, we use the standard inner product $\langle x, y \rangle$. We often work with linear operators $A\colon \ell^2 \to \ell^2$ and define the adjoint (or transpose) of A to be the operator A^* so that $\langle A x, y \rangle = \langle x, A^* y \rangle$ for all x and y in ℓ^2. Let $\pi(x)$ be a multivariate polynomial (with $x \in \mathbf{R}^d$). Let $\pi(\mathbf{Z}^d)$ (or π for short) be the sequence formed by evaluating this polynomial on the lattice $\mathbf{Z}^d$

$$\pi = \pi(\mathbf{Z}^d) = \{\pi(k) | k \in \mathbf{Z}^d\}.$$

We use Π_n to denote the space of all polynomial sequences of total degree strictly less than n.

B. One-Dimensional Filters

When a linear operator A is time invariant we call it a filter. Its action is convolution with the impulse response sequence $\{a_k | k \in \mathcal{K} = \mathbf{Z}\}$

$$(A x)_l = (a * x)_l = \sum_{k \in \mathcal{K}} a_{l-k} x_k.$$

In this work, we assume all impulse responses to be finite, that is, A is an FIR filter; therefore, the action of a filter on a polynomial sequence is well defined.

The z-transform of the impulse response sequence is a Laurent polynomial

$$A(z) = \sum_k a_k z^{-k}.$$

If we let $z = e^{i\omega}$ then $A(e^{i\omega})$ becomes the discrete-time Fourier transform of the impulse response. Note that we use capital letters to denote operators as well as Fourier transforms of sequences. The meaning will be clear from the context.

We often use differentiation with respect to ω to make statements about filters. It is convenient to define a scaled version of the differentiation operator as

$$\Delta = \frac{d}{i \, d\omega}.$$

We also combine this symbol with the z notation. Keep in mind that the differentiation is always with respect to ω and that z is nothing more than a place holder for $e^{i\omega}$. For example, z^{α} is simply $e^{i\alpha\omega}$ and there is no ambiguity even if α is a noninteger. Thus $\Delta z^{\alpha} = \alpha z^{\alpha}$ for all real α. We also define

$$\Delta^n A(z) = A^{(n)}(z) = \sum_k a_{-k} k^n z^k$$

so that

$$\Delta^n A(z^{\alpha}) = \alpha^n A^{(n)}(z^{\alpha}).$$

C. Multidimensional Filters

In the multidimensional setting ($\mathcal{K} = \mathbf{Z}^d$) we can use exactly the same machinery for dealing with filters as in the 1-D case as long as we use the multi-index notation. In other words, we think of an index $k \in \mathbf{Z}^d$ as a vector $(k_1, \cdots, k_d)$ where $k_j \in \mathbf{Z}$. Similarly we think of z as $(z_1, \cdots, z_d)$, n as $(n_1, \cdots, n_d)$ and α as $(\alpha_1, \cdots, \alpha_d)$. Now k^n and z^{α} have to be understood as

$$k^n = \prod_{j=1}^{d} k_j^{n_j}, \quad \text{and} \quad z^{\alpha} = \prod_{j=1}^{d} z_j^{\alpha_j}. \tag{1}$$

The size of a multi-index is

$$|n| = \sum_{j=1}^{d} n_j,$$

so that the degree of the monomial $x^n = x_1^{n_1} \cdots x_d^{n_d}$ is $|n|$. The differentiation operator is given by

$$\Delta^n = \frac{\partial^{|n|}}{i^{|n|} \, \partial \omega_1^{n_1} \cdots \partial \omega_d^{n_d}}.$$

If we adhere to these rules, it is still true, as in one dimension, that

$$\Delta^n A(z) = A^{(n)}(z) = \sum_k a_{-k} k^n z^k \quad \text{and}$$

$$\Delta^n A(z^{\alpha}) = \alpha^n A^{(n)}(z^{\alpha}). \tag{2}$$

Note that the above equations are vector equations. We will also use $\mathbf{1}$ to stand for $(1, \cdots, 1) \in \mathbf{Z}^d$.

D. Lattices and Sublattices

If D is a $d \times d$ matrix with integer coefficients, we can find a sublattice of $\mathcal{K} = \mathbf{Z}^d$ as $D\mathbf{Z}^d$. The determinant of D is an integer denoted by M, $|D| = M \in \mathbf{Z}$. Then there are $(M - 1)$

distinct cosets each of the form $D\mathbf{Z}^d + t_j$ with $t_j \in \mathbf{Z}^d$ and $1 \le j \le M - 1$. We know that

$$\mathbf{Z}^d = \bigcup_{j=0}^{M-1} (D\mathbf{Z}^d + t_j)$$

where $t_0 = 0$ and the union is disjoint. The t_j are unique if we restrict $D^{-1} t_j$ to be in the unit hypercube $[0, 1]^d$. Given a lattice $\mathcal{L} = \mathcal{D}\mathbf{Z}^d + t$, we can sample a polynomial on this lattice as

$$\pi(\mathcal{L}) = \{\pi(D\mathcal{K} + t) | \mathcal{K} \in \mathbf{Z}^d\}.$$

Note that $\pi(\mathcal{L}) \in \mathbf{R}^{\mathbf{Z}^d}$; hence, it is a sequence indexed by $\mathbf{Z}^d$ and not by $\mathcal{L}$. We also introduce $\downarrow D : \mathbf{R}^{\mathcal{K}} \to \mathbf{R}^{D\mathcal{K}}$ that is, the downsampling operator connected with the dilation matrix D. Its adjoint is the upsampling operator $\uparrow D$. To define upsampling in the z-domain we need to define z^D as

$$z^D = \{z^{d_1}, z^{d_2}, \cdots, z^{d_d}\}, \tag{3}$$

where d_i is the ith column vector of matrix D and z^{d_i} is as defined in (1).

So far, we only considered data sampled on the canonical lattice $\mathcal{K} = \mathbf{Z}^d$. Sometimes, however, the data is sampled on a more general lattice $\mathcal{K} = \Gamma \mathbf{Z}^d$, where Γ is an invertible $d \times d$ matrix. An example we will use in Section IV-A4 is the two-dimensional (2-D) triangular lattice where

$$\Gamma_{\text{triang}} = \begin{bmatrix} 1 & 1/2 \\ 0 & \sqrt{3}/2 \end{bmatrix}. \tag{4}$$

We can now find sublattices by premultiplying D by Γ. Given that our construction relies on polynomial interpolation and cancelation, and that polynomial spaces of fixed degree are invariant under affine transformations, we can, without loss of generality, assume that Γ is the identity. The only place where Γ plays a role is in choosing neighborhoods for the interpolants. We will come back to this in the examples.

E. Interpolating Filters

Definition 1: A multidimensional filter H is an interpolating filter if its impulse response satisfies $h_{Dk} = \delta_k$. For example, in one dimension with dilation 2, a filter is interpolating in case $h_{2k} = \delta_k$; this means the filter is zero in all even location except 0. Such filters are also called half band filters. In general, the filter has to be zero in all locations of the 0th coset $(D\mathbf{Z})$ except the origin. When applying an interpolating filter after upsampling, the values at the original sample locations are left unchanged and the values at the new sample locations are a linear combinations of the values at the old sample locations. To express an interpolating filter in the z-domain, sum the z-transform of h along all the cosets; on the $D\mathbf{Z}$ lattice (0th coset) only one term is nonzero. Thus, a filter is interpolating if its z-transform can be written as

$$H(z) = 1 + \sum_{i=1}^{M-1} z^{t_i} P_i(z^D)$$

where t_i are coset representatives. Such filters are called Mth band filters.

1) Multiresolution Analysis: In this section, we study the continuous-time setting. Consider a lattice $\mathcal{K} = \mathbf{Z}^d$ and the M sublattices induced by the dilation matrix D where $M = \text{D}$. Consider also a compactly supported scaling function $\varphi(x) \in L_2(\mathbf{R}^d)$ that satisfies the following refinement relation:

$$\varphi(x) = \sum_{k \in \mathcal{K}} h_k \, \varphi(D\,x - k)$$

where the h_k form the impulse response of a filter H. The translates and dilates of $\varphi(x)$ are defined as

$$\varphi_{j,k}(x) = M^{j/2} \varphi(D^j x - k) \quad \text{with} \quad k \in \mathcal{K} = \mathbf{Z}^d.$$

Using a vector function notation $\Phi_j = \{\varphi_{j,k} | k \in \mathcal{K}\}$ and the filter operations, we can express the refinement relations further as

$$\Phi_j = M^{-1/2} \mathbf{H} \, \Phi_{j+1}$$

where $\mathbf{H}$ is defined as $(\downarrow D) H$. We say that a scaling function is interpolating if it is one at the origin and zero on the other points of the lattice: that is, $\varphi(k) = \delta_k$. It is well known that if the scaling function is interpolating then the refinement filter H is interpolating as well. Note that the converse is not true.

We also consider a dual scaling function $\widetilde{\varphi}(x)$ and its translates and dilates which are biorthogonal to the primal scaling functions

$$\langle \widetilde{\varphi}_{j,k}, \, \widetilde{\varphi}_{j,k'} \rangle = \delta_{k-k'}.$$

We write the dual refinement relation as $\widetilde{\Phi}_j = M^{1/2} \widetilde{\mathbf{H}} \widetilde{\Phi}_{j+1}$, where $\widetilde{\mathbf{H}} = (\downarrow D) \widetilde{H}$. (Note the different normalization for the dual function.) Biorthogonality then implies that

$$\widetilde{\mathbf{H}} \mathbf{H}^* = 1.$$

Introduce now $M - 1$ wavelet functions $\psi_i \in L_2(\mathbf{R}^d)$ with $1 \le i \le M - 1$ and their translates and dilates $\psi_{i;j,k}$. The wavelet functions satisfy refinement relations given by

$$\Psi_{i;j} = M^{1/2} \mathbf{G}_i \, \Phi_{j+1}.$$

Our aim now is to find $\mathbf{H}$ and $\mathbf{G}_i$ so that the associated collection of wavelets

$$\psi_{i;j,k}(x) \quad \text{with} \quad j \in \mathbf{Z}, \quad k \in \mathcal{K}, \quad 1 \le i \le M - 1$$

forms an unconditional basis for $L_2(\mathbf{R}^d)$. Dual wavelets $\widetilde{\Psi}_i$ exist as well and they also satisfy refinement relations with $\widetilde{\mathbf{G}}_i$. The dual wavelets are biorthogonal to the primal wavelets so that the expansion of a function $f \in L(\mathbf{R}^d)$ can be found as

$$f = \sum_{j \in \mathbf{Z}} \sum_{k \in \mathcal{K}} \sum_{i=0}^{M-1} \langle \widetilde{\psi}_{i;j,k}, f \rangle \psi_{i;j,k}.$$

Wavelet expansions are efficient in the sense that for a large class of functions, the majority of the wavelet coefficients will be small. In particular for smooth functions f, the error of the
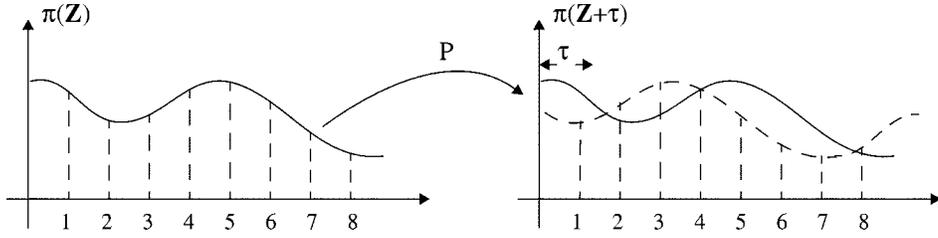
Fig. 1. Suppose we are given a polynomial π of order $n < N$ sampled on the lattice of integers $\mathbf{Z}$. A Neville filter P of order N applied to this sampled sequence (points on the solid line) results in a sequence that can be obtained by sampling the same polynomial, just offset by τ (points on the dashed line).

wavelet expansions decays as $M^{-j\widetilde{N}}$ where $\widetilde{N}$ is the number of vanishing moments of the dual wavelets, that is

$$\int x^p \, \widetilde{\psi}_i(x) \, dx = 0 \quad \text{for } |p| < \widetilde{N}.$$

This is equivalent to the primal scaling functions being able to reproduce polynomials up to degree $\widetilde{N}$ exactly. Similarly, the primal wavelet has N vanishing moments and the dual scaling functions can reproduce polynomials up to degree N. In Section III, we go into more detail on the interaction of filter banks with polynomials.

The above properties of the scaling function and wavelets can be easily translated to the filter sequences of the refinement relations. The vanishing moments conditions imply that $(1 \le i \le M - 1)$

$$\begin{aligned} \widetilde{\mathbf{G}}_i \, \pi &= 0, \quad \text{for } \pi \in \Pi_{\widetilde{N}}, \quad \text{and} \\ \mathbf{G}_i \, \pi &= 0, \quad \text{for } \pi \in \Pi_N. \end{aligned} \tag{5}$$

These conditions are sometimes referred to as "sum rules" and are closely related to the approximation order of the scaling function [24].

The biorthogonality requirements imply that

$$\mathbf{H}^* \, \widetilde{\mathbf{H}} + \sum_{i=1}^{M-1} \mathbf{G}_i^* \, \mathbf{G}_i = 1. \tag{6}$$

2) Convergence and Smoothness of Scaling Functions: A multiresolution analysis implies the existence of a perfect reconstruction filter bank with filters H, $\widetilde{H}$, G, and $\widetilde{G}$. On the other hand, given a perfect reconstruction filter bank, an associated multiresolution analysis may not always exist, i.e., the wavelets may not form a stable basis or even belong to L_2. The existence of a basis depends on the spectrum of the transfer operator $\mathbf{T}$ and the dual transfer operator $\widetilde{\mathbf{T}}$, where

$$\mathbf{T} = (\downarrow D) \, M^{-1} \, H \, H^* \quad \text{and} \quad \widetilde{\mathbf{T}} = (\downarrow D) \, M \, \widetilde{H} \, \widetilde{H}^*. \tag{7}$$

The following result is known.

Theorem 2: If N and $\widetilde{N}$ are at least one and the transfer operator and dual transfer operator have all eigenvalues $|\lambda| < 1$ except for a simple eigenvalue $\lambda = 1$, then an associated multiresolution and a stable biorthogonal wavelet basis exist.

This combines results relating the stability of the wavelet basis to the Sobolev regularity of the functions [12] and results relating the Sobolev regularity to the spectrum of the transfer operator [9], [25], [40]. If the filters are FIR, then this condition

can be checked by computing the eigenvalues of a finite matrix, the size of which depends on the length of the filters.

To actually compute the Sobolev regularity, we need to find the transfer operator $\mathbf{T}$ and its invariant submatrix $\mathbf{T}_r$. Then we compute the eigenvalues of $\mathbf{T}_r$ and use the fact that an estimate of the lower bound on the Sobolev exponent is given by [9]

$$\frac{\log \rho}{2 \log \lambda_{\max}} \le s \le \frac{\log \rho}{2 \log \lambda_{\min}} \tag{8}$$

where $\lambda_{\max}$, $\lambda_{\min}$ are the maximum and minimum eigenvalues of the dilation matrix, respectively, and ρ is the maximum non-special eigenvalue of $\mathbf{T}_r$. Special eigenvalues are eigenvalues that correspond to a polynomial left eigenvector (see [47] for a discussion of the role of special eigenvalues).

III. NEVILLE FILTERS

We introduce a class of filters which is crucial in the constructions of filter banks and wavelets using lifting. Since these filters are closely connected to polynomial interpolation, we call them Neville filters in honor of Neville and his algorithm for 1-D polynomial interpolation, see, e.g., [46]. We show how Neville filters generalize well-known filters such as Coiflets and Deslauriers-Dubuc filters.

A Neville filter applied to a polynomial sampled on a lattice results in that same polynomial, but now sampled on the original lattice offset by τ (see Fig. 1). More precisely, we have the following.

Definition 3: A filter P is a Neville filter of order N with shift $\tau \in \mathbf{R}^d$ if

$$P \, \pi(\mathbf{Z}^d) = \pi(\mathbf{Z}^d + \tau), \quad \text{for } \pi \in \Pi_N. \tag{9}$$

Note that τ need not be an integer vector.

Consider a simple example of a linear polynomial $\pi(t) = t + a$ sampled on the integers $\pi(\mathbf{Z}) = k + a, k \in \mathbf{Z}$. We show that the filter P with $p_0 = p_{-1} = 1/2$ is a Neville filter of order 2 with shift $1/2$. To that end, we convolve $\pi(\mathbf{Z})$ with P as in (9) (we perform the convolution in the z-domain since it then amounts to simple multiplication)

$$\begin{aligned} P(z) \cdot \Pi(z) &= (1/2 + 1/2 z) \cdot \sum_k (k + a) \cdot z^{-k} \\ &= \tfrac{1}{2} \sum_k (2k + 2a + 1) \cdot z^{-k} \\ &= \sum_k (k + a + 1/2) \cdot z^{-k}. \end{aligned}$$

This last expression is the z-transform of $\pi(\mathbf{Z} + 1/2)$ which means that P is a Neville filter with shift $1/2$. Let us find the equivalent of (9) in terms of the impulse response $\{p_k\}$. Substitute a monomial x^n into (9)

$$\sum_k p_{-k} (l+k)^n = (l+\tau)^n \quad \text{for } |n| < N.$$

Given that polynomial spaces are shift invariant it is sufficient to consider $l = 0$

$$\sum_k p_{-k} k^n = \tau^n, \quad \text{for } |n| < N \tag{10}$$

where according to (2), the left-hand side is equal to $P^{(n)}(\mathbf{1})$. We thus showed the following proposition.

Proposition 4: A filter P is a Neville filter of order N with shift τ if and only if its impulse response satisfies

$$\sum_k p_{-k} k^n = P^{(n)}(\mathbf{1}) = \tau^n, \quad \text{for } |n| < N.$$

Continuing our simple example from above, let us check the condition of Proposition 4. We need to show that

$$\sum_k p_{-k} k^n = (\tfrac{1}{2})^n, \quad \text{for } |n| < 2.$$

We have that

$$n = 0: \quad p_0 \cdot 0^0 + p_{-1} \cdot 1^0 = \tfrac{1}{2} + \tfrac{1}{2} = 1 = (\tfrac{1}{2})^0,$$
$$n = 1: \quad p_0 \cdot 0^1 + p_{-1} \cdot 1^1 = 0 + \tfrac{1}{2} = \tfrac{1}{2} = (\tfrac{1}{2})^1.$$

Note that the scalar multiple of a Neville filter is not a Neville filter. The next proposition shows that the adjoint of a Neville filter, that is, the filter obtained by time-reversing its impulse response and thus replacing z with z^{-1}, is a Neville filter as well.

Proposition 5: If P is a Neville filter of order N with shift τ, then P^* is a Neville filter of order N with shift $-\tau$.

Proof: Let q be the impulse response of P^*. Then $Q(z) = P(z^{-1})$. Given that $\Delta z^{-1} = -z^{-1}$, it follows from Proposition 4 that

$$Q^{(n)}(\mathbf{1}) = (-1)^{|n|} P^{(n)}(\mathbf{1}) = (-\tau)^n \quad \text{for } |n| < N.$$

∎

The following proposition shows how Neville filters interact:

Proposition 6: If P is a Neville filter of order N with shift τ, and P' is a Neville filter of order N' with shift τ', then $P P'$ is a Neville filter of order $\min(N, N')$ with shift $\tau + \tau'$.

Proof: The proof is left as an exercise to the reader. ∎
Proposition 6 also shows that the Neville filters of a fixed order form an Abelian group. We conclude by showing how Neville filters interact with upsampling.

Proposition 7: If P is a Neville filter of order N with shift τ, then $Q(z) = P(z^D)$ is a Neville filter of order N with shift $D\tau$.

A. Examples of Neville Filters

Here we consider some well-known filters that fit into the definition of Neville filters.

TABLE I
DESLAURIERS–DUBUC FILTERS FOR
ORDERS 1 TO 8. THESE FILTERS ARE THE SHORTEST NEVILLE FILTERS WITH
SHIFT $1/2$. THE EVEN ORDER ONES ARE THE MOST INTERESTING AS
THEY HAVE LINEAR PHASE

	Numerator								Denominator
$N \setminus k$	3	2	1	0	−1	−2	−3	−4	
1				1					1
2				1	1				2
3			3	6	−1				2^3
4			−1	9	9	−1			2^4
5		−5	60	90	−20	3			2^7
6		3	−25	150	150	−25	3		2^8
7	−5	42	−175	700	525	−70	7		2^{10}
8	−5	49	−245	1225	1225	−245	49	−5	2^{11}

1) The identity filter, where the impulse response is a Kronecker delta pulse, is obviously a Neville filter of order infinity with shift 0. Similarly, a monomial filter z^k with $k \in \mathbf{Z}^d$ is a Neville filter of order infinity with shift k. This shows that we only need to worry about building Neville filters with shifts in the unit hypercube. Any other shift can be obtained by multiplying the original Neville filter with the correct power of z.

2) Deslauriers-Dubuc interpolating subdivision uses filters which can predict the values of a polynomial at the half integers given the polynomial at the integers [19]. Hence these filters are Neville filters with shift $1/2$. As an example, let us construct a Neville filter of order $N = 4$ by solving the following set of equations:

$$\sum_{k=-2}^{1} p_{-k} k^n = 1/2^n, \quad \text{for } 0 \le n < 4$$

leading to $P^4(z) = (-z + 9 + 9z^{-1} - z^{-2})/16$. Table I gives the Deslauriers–Dubuc filters up to order 8.

3) We saw that interpolating filters H can be written as $H(z) = 1 + z^{-1} P(z^2)$. If P is a Neville filter of shift $1/2$, as are the Deslauriers-Dubuc filters, then we can use the earlier propositions to see that H is a Neville filter of the same order and shift 0. Given that $H(z) + H(-z) = 2$, H has the same number of zeros at $z = -1$. Thus H is a Lagrangian halfband filters as defined in [56].

4) Every FIR filter is a Neville filter of order 2 with the shift equal to the first moment $\tau = H^{(1)}(1)$.

5) The lowpass orthogonal Daubechies filters [13] of order 2 or more satisfy $H^{(2)}(1) = (H^{(1)}(1))^2$ [22]. In fact, this is true for any orthogonal lowpass filters of order at least 2 [50]. Consequently, these filters are Neville filters of order 3 with shift their first moment $H^{(1)}(1)$.

6) Coiflets are filters H with zero moments up to N, excluding the zero*th* moment which is one, $H^{(n)}(1) = \delta_n$ for $n < N$ [14]. They are thus Neville filters of order N with shift zero. Consequently, polynomials of degree less than N are eigenfunctions of Coiflets. Using Propositions 5 and 6 we see that the autocorrelation of any Neville filter is a Coiflet of the same order.

7) Neville filters are closely connected to the one-point quadrature formula from [50]; If a Neville filter has order N, then the one-point quadrature formula for the
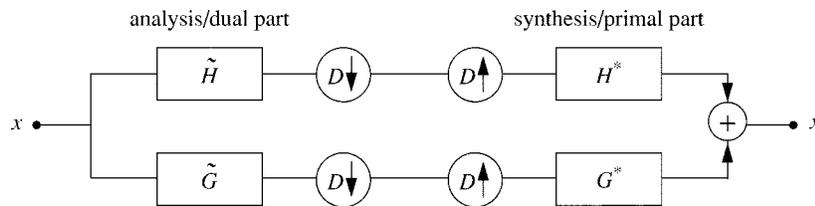
Fig. 2. The d-dimensional two-channel analysis/synthesis filter bank.

corresponding scaling function has degree of accuracy $N + 1$.

8) The ideal Neville filter with shift τ and order infinity is the allpass filter z^τ. However it is not an FIR filter unless τ is an integer vector. One has to be extremely careful by applying such a filter to a polynomial sequence as the summation converges only conditionally. These filters are thus of limited practical use but can be thought of as the limiting case for FIR Neville filters with fixed τ as N goes to infinity.

B. Construction of Neville Filters

Building Neville filters in d dimensions with a certain pre-scribed order N and shift τ reduces to polynomial interpolation. There are

$$q = \binom{N + d - 1}{d} \tag{11}$$

equations like (10) to satisfy, so one would expect we need $f = q$ filter taps. To avoid extrapolation one should choose the f filter taps in the neighborhood of τ. The Neville filter can the be found by solving a $q \times q$ linear system. In one dimension, this system has a Vandermonde matrix and is always invertible. This leads to classic Lagrangian interpolation; Neville's algorithm [46] provides a fast way of computing the interpolant at a given point.

In higher dimensions, the situation is more complex and the linear system is not always solvable. It can either be overdeter-mined or underdetermined; thus, to achieve order N one may need either more than q or less than q filter taps. For example, consider three points (x_1, y_1), (x_2, y_2), (x_3, y_3) in the plane $\mathbf{R}^2$, each with an associated function value z_1, z_2 and z_3. One would expect there to be a unique plane, given by a linear poly-nomial $z = ax + by + c$ that interpolates these points. However, in case the three points (x_1, y_1), (x_2, y_2), (x_3, y_3) are collinear, infinitely many such planes exist. In this case the interpolation problem reduces to a 1-D problem along the common line the three points are on. In this direction, a unique *quadratic* and *single variable* interpolating polynomial exists. This then can be extended to a unique solution in two dimensions by letting the polynomial be constant in the direction orthogonal to the common line.

This example shows that the degree of interpolation depends not only on the *number* of interpolation points but also on their *geometric configuration*. It is not clear a priori how many inter-polation points and which geometric configurations are needed to uniquely solve the interpolation problem for a space of poly-nomials up to a certain degree. de Boor and Ron provide an elegant solution by posing the question differently [17], [18].

As opposed to fixing the degree of the polynomial space and then asking which configurations are possible, they fix a con-figuration of points and then find a space of polynomials in which to solve the interpolation problem. The particular space depends on the configuration of the points, but for any values at the points, there is a unique interpolating polynomial from the space. An efficient algorithm to evaluate this polynomial exists.

To construct Neville filters, we follow the same strategy. We first fix a neighborhood of points around τ and use the de Boor–Ron algorithm to compute the space in which the interpolation problem can be solved. The order N is then found as the largest N for which Π_N belongs to the space. If we want to get a larger N, we enlarge the original neighborhood until the desired N is obtained.

IV. TWO-CHANNEL INTERPOLATING FILTER BANKS

To simplify the exposition, we first consider two-channel filter banks. Once the construction in the two-channel case is clear the M-channel case can easily be understood.

The framework for a two-channel filter bank is depicted in Fig. 2. It involves two analysis filters $\widetilde{H}$ (lowpass) and $\widetilde{G}$ (high-pass) and two synthesis filters H (lowpass) and G (highpass). As before, let

$$\mathbf{H} = (\downarrow D)\, H, \qquad \mathbf{G} = (\downarrow D)\, G$$

and similarly for the duals. Consequently, $\mathbf{H}^* = H^* (\uparrow D)$. We want to obtain a perfect reconstruction filter bank, that is, analysis followed by synthesis gives the identity

$$\mathbf{H}^*\, \widetilde{\mathbf{H}} + \mathbf{G}^*\, \widetilde{\mathbf{G}} = 1 \tag{12}$$

and synthesis followed by analysis is the identity as well. In other words,

$$\widetilde{\mathbf{H}}\, \mathbf{H}^* = 1, \quad \widetilde{\mathbf{H}}\, \mathbf{G}^* = 0, \quad \widetilde{\mathbf{G}}\, \mathbf{H}^* = 0, \quad \widetilde{\mathbf{G}}\, \mathbf{G}^* = 1.$$

This implies that $\mathbf{H}^*\, \widetilde{\mathbf{H}}$ is a projection operator and the filter bank thus corresponds to a splitting in complementary sub-spaces. Note that the perfect reconstruction condition for filter banks is identical to the necessary condition for biorthogonality (6).

A. Vanishing Moments

How does a filter bank interact with polynomial sequences? Since all filters are FIR, we can let them act on polynomial se-quences. This will lead to the definition of two important charac-teristics of a filter bank: the number of primal (N) and dual $(\widetilde{N})$ vanishing moments. These correspond to the degree of polyno-mials which are annihilated by the highpass filters, as in (5).
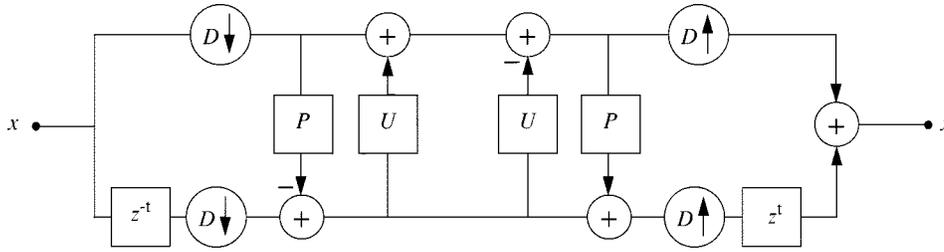
Fig. 3.   The lifting scheme. P and U stand for prediction and update operators, respectively.

Definition 8: We say that a filter bank has N primal and $\widetilde{N}$ dual vanishing moments if

$$\mathbf{G}\,\pi = 0 \quad \text{for } \pi \in \Pi_N, \quad \text{and}$$
$$\widetilde{\mathbf{G}}\,\pi = 0 \quad \text{for } \pi \in \Pi_{\widetilde{N}}. \tag{13}$$

Using perfect reconstruction (12), one can see that the dual moment condition implies that $\mathbf{H}^* \widetilde{\mathbf{H}} \pi = \pi$. Indeed, if the highpass filter kills polynomials, these polynomials have to be preserved in the lowpass branch of the system. Similarly the primal moment condition implies that $\pi^* \mathbf{H}^* \widetilde{\mathbf{H}} = \pi^*$. The number of primal vanishing moments concerns the degree of the moments of an input sequence that are preserved by the lowpass branch, or, equivalently, the number of zero moments of elements in the highpass branch. Indeed, it makes obvious sense for the mean or DC component of the signal to appear only in the lowpass branch. In summary, we want to build filter banks that have the following three properties:

1) PR: Perfect reconstruction property as given in (12);
2) DM: Dual vanishing moments as given in (13);
3) PM: Primal vanishing moments as given in (13).

In the next section, we show how lifting allows us to obtain these properties.

B. Lifting

Several methods have been introduced in the literature to build filter banks that satisfy PR, DM, and PM. Typically, they try to satisfy all three conditions at once which may lead to cumbersome algebraic conditions, especially in high dimensions.

The main feature of lifting is that it allows us to satisfy each condition separately. First, every filter bank built with lifting automatically satisfies PR. Most often, we build a filter bank starting from a trivial filter bank and then we enhance its properties using lifting steps. In this paper, two lifting steps will suffice: the first one, called predict, ensures that DM is satisfied, while the second one, called update, ensures that PM is satisfied. We show how each step can be designed separately.

The trivial filter bank we use to start lifting is the polyphase transform which splits the signal into even- and odd-indexed components as in Fig. 3. The result is that the filter bank which is not time invariant because of downsampling, becomes time invariant in the polyphase domain. In the first lifting step, we use a predict filter P to predict the odd samples from the even ones. The even samples remain unchanged, while the result of the predict filter applied to the even samples is subtracted from the odd samples yielding the highpass or wavelet coefficients.

Here, we design the P filter so that if the input sequence is a polynomial sequence, then the prediction of the odd samples is exact, highpass coefficients are zero and DM is satisfied. In the second step, we use an update filter U to update the even samples based on the previously computed highpass or wavelet coefficients. Here we design U to satisfy PM.

To start, use Fig. 3 to identify the polyphase matrix as

$$\mathcal{P} = \begin{bmatrix} \widetilde{H}_e & \widetilde{H}_o \\ \widetilde{G}_e & \widetilde{G}_o \end{bmatrix} = \begin{bmatrix} 1 & U \\ 0 & 1 \end{bmatrix} \begin{bmatrix} 1 & 0 \\ -P & 1 \end{bmatrix}$$
$$= \begin{bmatrix} 1 - UP & U \\ -P & 1 \end{bmatrix}. \tag{14}$$

The inverse adjoint polyphase matrix is

$$\mathcal{P}^{*\,-1} = \begin{bmatrix} H_e & H_o \\ G_e & G_o \end{bmatrix} = \begin{bmatrix} 1 & P^* \\ -U^* & 1 - U^* P^* \end{bmatrix}. \tag{15}$$

From the polyphase decomposition we can find the filter H as

$$H(z) = H_e(z^D) + z^t H_o(z^D).$$

Note that H is interpolating since $H_e(z) = 1$. The DM condition now becomes

$$\widetilde{\mathbf{G}}\,\pi(\mathbf{Z}^d) = \widetilde{G}_e\,\pi(D\,\mathbf{Z}^d) + \widetilde{G}_o\,\pi(D\,\mathbf{Z}^d + t) = 0.$$

Substituting values from the polyphase matrix (14) yields

$$P\,\pi(D\,\mathbf{Z}^d) = \pi(D\,\mathbf{Z}^d + t). \tag{16}$$

Given that this has to hold for all $\pi \in \Pi_{\widetilde{N}}$ and that the space $\Pi_{\widetilde{N}}$ is invariant under D, the above equation is equivalent to

$$P\,\pi(\mathbf{Z}^d) = \pi(\mathbf{Z}^d + D^{-1} t), \quad \text{for } \pi \in \Pi_{\widetilde{N}}. \tag{17}$$

Thus, to satisfy DM, P has to be a Neville filter of order $\widetilde{N}$ and shift $\tau = D^{-1} t$. This connects to the intuition behind the predict operator. If we input a polynomial sequence of degree less than $\widetilde{N}$, then all highpass coefficient (lower branch in Fig. 3) have to be zero to obtain vanishing moments. This implies that the prediction is always exact. Thus, the predict filter applied to a polynomial sampled on the "even" lattice $D\,\mathbf{Z}^d$ has to result in the same polynomial on the "odd" lattice $D\,\mathbf{Z}^d + t$. This is precisely (16).

Similarly, to satisfy PM, use (15) to get

$$\mathbf{G}\,\pi(\mathbf{Z}^d) = G_e\,\pi(D\,\mathbf{Z}^d) + G_o\,\pi(D\,\mathbf{Z}^d + t)$$
$$= -U^*\pi(D\,\mathbf{Z}^d) + (1 - U^* P^*)\,\pi(D\,\mathbf{Z}^d + t) = 0$$

for $\pi \in \Pi_N$. We already know that P is a Neville filter of order $\widetilde{N}$ and shift τ. Thus, if $N \leq \widetilde{N}$ we use (17) to obtain

$$-U^* \pi(D\mathbf{Z}^d) + \pi(D\mathbf{Z}^d + t) - U^* \pi(D\mathbf{Z}^d) = 0,$$
$$\text{for } \pi \in \Pi_N$$

or

$$2U^* \pi(D\mathbf{Z}^d) = \pi(D\mathbf{Z}^d + t).$$

Therefore, $2U$ has to be a Neville filter of order N with shift $-\tau = -D^{-1}t$. A natural choice is to let U be the adjoint of a predict filter with order N divided by 2. We now have the following theorem.

Theorem 9: Let $N \leq \widetilde{N}$. We can build a filter bank with N primal vanishing moments and $\widetilde{N}$ dual vanishing moments by letting the predict filter be a Neville filter of order $\widetilde{N}$ with shift $\tau = D^{-1}t$ and choosing the update filter as half the adjoint of a Neville filter of order N and shift τ.

Remarks:

1) The theorem results in a Neville filter $P^{\widetilde{N}}$ with shift $\tau = D^{-1}t$ and the update $U = P^{N*}/2$ which is a multiple of a Neville filter P^{N*} with shift $-\tau = -D^{-1}t$. Note that U per se is not a Neville filter.

2) The condition $N \leq \widetilde{N}$ is not very restrictive. In image compression it is known that the number of dual moments is more important than the number of primal moments. The dual moments take care of polynomial cancelation as well as of the smoothness of the primal functions. If, for some reason, one would need $N > \widetilde{N}$, one can always exchange the role of the primal and dual filters. In that case the *analysis* lowpass filter is interpolating and the analysis functions are smooth.

3) While the connection between the predict and Neville filters is intuitively clear, there is much less intuition behind the update filter. The purpose of the update operator is to turn the "even" samples into lowpass samples which have the same average as the original sequence. The average of two numbers is always one number plus *one half* times the difference. This explains why a factor $1/2$ is needed. To get the same effect for higher order polynomials, we need Neville filters. Given that the "odd" grid $D\mathbf{Z}^d + t$ can be obtained from the "even" grid $D\mathbf{Z}^d$ by a relative shift of $-\tau$ it is natural that an *adjoint* Neville filter is needed.

C. Examples of Two-Channel Interpolating Filter Bank Families

1) Haar: To build a filter bank in one dimension with $N = \widetilde{N} = 1$, we need the simplest predict and update filters: $P(z) = 1$ and $U(z) = 1/2$. This results in the filters $H(z) = 1 + z^{-1}$ and $G(z) = -1/2 + z^{-1}/2$, that form the unnormalized Haar filter bank.

2) One-Dimensional Filter Bank Families of Higher Order: Let us now construct 1-D filter bank families with N primal and $\widetilde{N}$ dual vanishing moments, where $N \leq \widetilde{N}$. As an example, we let predict be P^4 and update $P^{2*}/2$ from Table I, and thus according to Theorem 9

$$P(z) = P^4(z) = (-z + 9 + 9z^{-1} - z^{-2})/16,$$
$$U(z) = 1/2\, P^{2*}(z) = (z+1)/4.$$
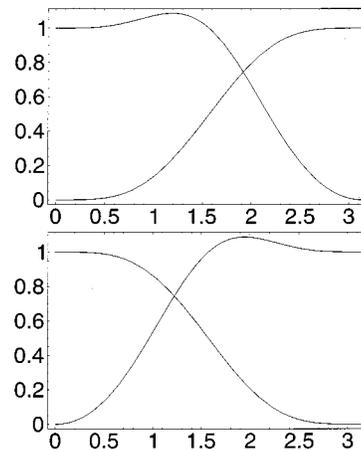
Fig. 4. Two-channel 1-D case: magnitude Fourier transforms of the analysis/synthesis filter pairs, for the example with $\widetilde{N} = 4$ dual and $N = 2$ primal vanishing moments. Note how the four dual vanishing moments make the dual (analysis) highpass filter smoother at the origin than the primal (synthesis) highpass filter.

We now have the complete system according to Fig. 3. To find the actual filters as in Fig. 2, we use (14) for the dual/analysis filters yielding

$$\begin{aligned}
\widetilde{H}(z) &= \widetilde{H}_e(z^2) + z^{-1}\widetilde{H}_o(z^2) \\
&= (z^4 - 8z^2 + 16z + 46 + 16z^{-1} - 8z^{-2} + z^{-4})/64 \\
&= (1 + z^{-1})^2(z^4 - 2z^3 - 5z^2 \\
&\quad + 28z - 5 - 2z^{-1} + z^{-2})/64.
\end{aligned}$$

Similarly, for the primal/synthesis filters we use (15)

$$\begin{aligned}
H(z) &= (-z^3 + 9z + 16 + 9z^{-1} - z^{-3})/16 \\
&= -(1 + z^{-1})^4(z^3 - 4z^2 + z)/16.
\end{aligned}$$

The factorizations of $\widetilde{H}(z)$ and $H^*(z)$ given above demonstrate that we indeed have 2 primal and 4 dual vanishing moments since there are 2 and 4 zeros at $z = -1$ in $\widetilde{H}(z)$ and $H^*(z)$, respectively, which is equivalent to having 2 and 4 zeros at $z = 1$ in $G^*(z)$ and $\widetilde{G}(z)$, respectively. Note also that the primal/synthesis lowpass filter H^* is interpolating. The magnitude Fourier transforms of the analysis/synthesis pairs are given in Fig. 4. Note how the analysis highpass filter is smoother at the origin than the synthesis highpass.

Using Theorem 9, one can build the entire biorthogonal wavelet family from [48]. These wavelets can be thought of as biorthogonal Coiflets; they were also derived independently, but without the use of lifting, by Reissell [35], Tian and Wells [52], and Strang [47].

3) Shannon: The limiting case of the 1-D family uses the ideal Neville filter $P(z) = z^{1/2}$. Given that

$$z^{1/2} = \sum_k \frac{(-1)^k}{\pi(k + 1/2)} z^{-k}$$

we see that $H(z) = 1 + z^{-1}P(z^2)$ is the ideal Shannon filter of height 2 on $[-\pi/2, \pi/2]$. Similarly let $U(z) = 1/2\,z^{-1/2}$, leading to $P(z)U(z) = 1/2$ and $G(z) = 1/2\,z^{-1/2} + 1/2$. Thus, this is the ideal Shannon filter of height $1/2$ on $[-\pi, -\pi/2] \cup [\pi/2, \pi]$. We thus recover the ideal filter bank or Shannon wavelet up to a normalization constant. The 1-D family from Section III-C2 thus forms a natural bridge between
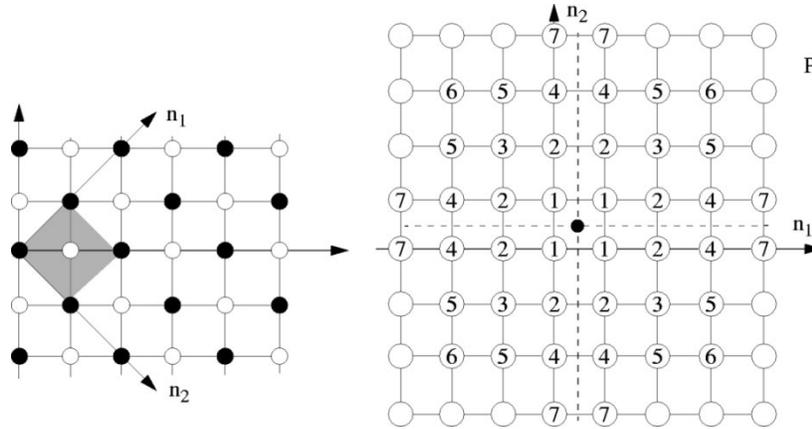
Fig. 5. Quincunx lattice with its units cell and the lattice in the sampled domain with neighborhoods. The small black dot within the first ring is the point $\tau = (1/2, 1/2)$ at which we want to interpolate.

that Haar and the Shannon wavelets. Note that both of these are orthogonal while the other members of the family are biorthogonal.

4) Causal Lifting: Using polynomial extrapolation instead of interpolation, it is possible to build both causal and anticausal Neville filters. By letting the predict be a causal Neville, and the update be the adjoint of an anticausal Neville filter, it is possible to build a filter bank with only causal lifting steps.

For example, a causal predict filter of order 2 is given by

$$P_{\text{causal}}(z) = -1/2 \, z^{-1} + 3/2$$

while an anticausal predict of order 2 is given by

$$P_{\text{anticausal}}(z) = 1/2 + 1/2 \, z.$$

Thus, by taking P_{causal} as the predict and $1/2 P^*_{\text{anticausal}} = 1/4 z^{-1} + 1/4$ as the update, we can build a causal transform with two primal and two dual moments. Note that in this example the predict filter uses extrapolation and there is no associated continuous scaling function. This is a very simple example. To get practically useful causal filters, we would need many more filter taps.

Upon finishing this paper, we learned of the work of Schuller [41], [42] concerning low-delay filter banks and applications in audio coding. This work, done independently from lifting, fits into the lifting framework and illustrates another feature of lifting, namely minimal-delay filter banks. It is known that a filter bank with causal filters only typically achieves perfect reconstruction only up to a delay. In several applications, particularly audio coding, delay is undesirable. Orthogonal filter banks have delay proportional to the length of the filters. With lifting, however, one can build polyphase matrices with determinant one that contain only causal filters. Consequently, the inverse polyphase matrix has causal filters as well and the filter operations do not introduce any delay. The only delay in the system comes from the polyphase representation and is proportional only to the number of subbands. Moreover, lifting completely characterizes all filter banks with minimal delay.

5) Quincunx Interpolating Filter Bank Families: The quincunx lattice is a 2-D nonseparable lattice with $M = 2$. One of the possible dilation matrices is given by

$$D = \begin{pmatrix} 1 & 1 \\ 1 & -1 \end{pmatrix}$$

TABLE II
QUINCUNX NEVILLE FILTERS. THE RINGS CORRESPOND TO RINGS GIVEN IN FIG. 5. THE NUMBERS IN PARENTHESES GIVE THE NUMBER OF POINTS IN EACH RING

Taps	Order \ Ring	Numerator							Denominator
		1(4)	2(8)	3(4)	4(8)	5(8)	6(4)	7(8)	
4	2	1							2^2
12	4	10	-1						2^5
24	6	174	-27	2	3				2^9
44	8	23300	-4470	625	850	-75	9	-80	2^{16}

also called the "symmetry" matrix. Fig. 5 depicts the quincunx lattice together with its unit cell and the coset representative. Since coset representatives come from the unit square it follows that $t_1 = (1, 0)$. According to Theorem 9, the shift for the Neville filters is $\tau = D^{-1} t_1 = (1/2, 1/2)$ (see Fig. 5). We choose different sizes of symmetric neighborhoods around τ and use the de Boor-Ron algorithm to compute the interpolation order and weights for the predict P. The results are given in Table II.

As an example, let us again construct a filter bank with $\widetilde{N} = 4$ and $N = 2$. According to Theorem 9

$$\begin{aligned}
P(z_1, z_2) &= P^4(z_1, z_2) \\
&= (10 * (1 + z_1^{-1} + z_2^{-1} + z_1^{-1} z_2^{-1}) \\
&\quad - (z_1^{-2} + z_2^{-2} + z_1^{-2} z_2^{-1} + z_1^{-1} z_2^{-2} \\
&\quad + z_1 + z_2 + z_1 z_2^{-1} + z_1^{-1} z_2)) / 2^5
\end{aligned}$$

where the update U is $P^{2*}/2$ and thus

$$U(z_1, z_2) = P^2(1/z_1, 1/z_2)/2 = (1 + z_1 + z_2 + z_1 z_2)/2^3.$$

Then, the actual dual/analysis filters from Fig. 2 are given by

$$\begin{aligned}
\widetilde{H}(z_1, z_2) &= \widetilde{H}_e(z^D) + z^{-t_1} \widetilde{H}_o(z^D) \\
&= \widetilde{H}_e(z_1 z_2, z_1/z_2) + z^{-t_1} \widetilde{H}_o(z_1 z_2, z_1/z_2), \\
\widetilde{G}(z_1, z_2) &= \widetilde{G}_e(z_1 z_2, z_1/z_2) + z^{-t_1} \widetilde{G}_o(z_1 z_2, z_1/z_2).
\end{aligned}$$

Using (14) we finally obtain

$$\begin{aligned}
\widetilde{H}(z_1, z_2) &= 1 - U(z_1 z_2, z_1/z_2) P(z_1 z_2, z_1/z_2) \\
&\quad + z_1^{-1} U(z_1 z_2, z_1/z_2), \\
\widetilde{G}(z_1, z_2) &= 1 - P(z_1 z_2, z_1/z_2).
\end{aligned}$$

(a)

(b)
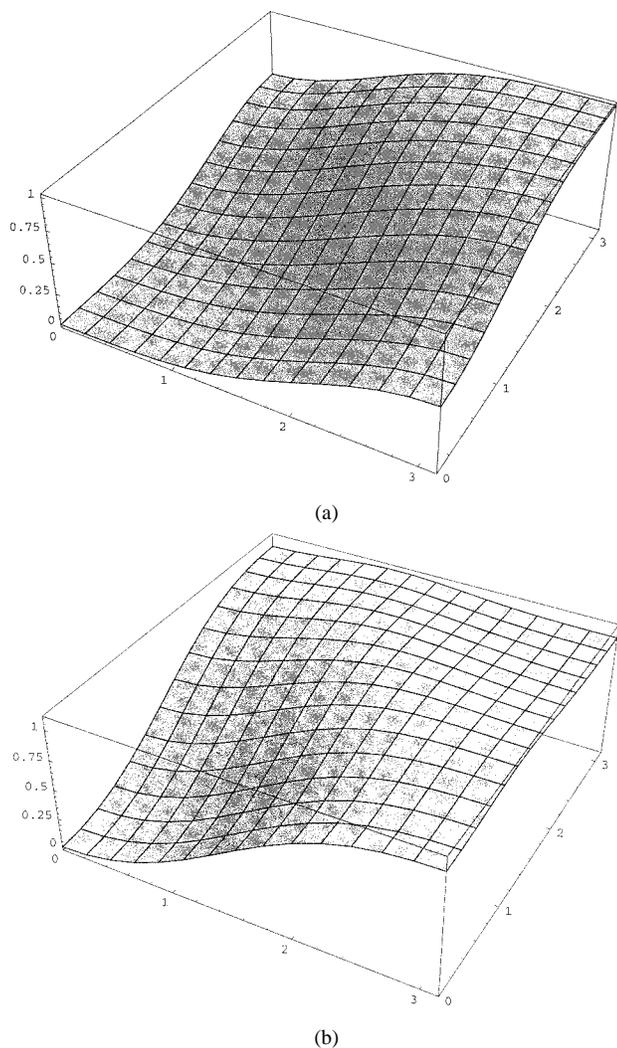
Fig. 6. Two-channel 2-D quincunx case: magnitude Fourier transforms of the analysis/synthesis highpass filters with $\widetilde{N} = 4$ dual and $N = 2$ primal vanishing moments. The four dual vanishing moments make the dual (analysis) highpass filter a much smoother function at the origin than the primal (synthesis) highpass filter.

(a)

(b)

Fig. 7. Two-channel 2-D quincunx case: fifth iteration of the primal and dual wavelets with $\widetilde{N} = 4$ dual and $N = 2$ primal vanishing moments, respectively. Note that this combination does not lead to a stable biorthogonal basis, as given by Sobolev regularity in Table III.

TABLE III
SOBOLEV REGULARITY OF SCALING FUNCTIONS. THE FIRST ROW GIVES THE REGULARITY OF THE PRIMAL SCALING FUNCTION OF A GIVEN ORDER $\widetilde{N}$ (2 THROUGH 8) WHILE THE REMAINING ROWS GIVE REGULARITIES OF DUAL SCALING FUNCTION WITH ORDER $N \leq \widetilde{N}$. NEGATIVE VALUES MEAN THAT THE BIORTHOGONAL BASIS IS NOT STABLE. FOR EXAMPLE, THE PAIR $(\widetilde{N}, N) = (4, 4)$ GIVES A STABLE BIORTHOGONAL BASIS. NOTE HOW REGULARITY INCREASES BOTH WITH N AND $\widetilde{N}$

$N \setminus \tilde{N}$	2	4	6	8
	1.577646	2.447930	3.154570	3.777470
2	−0.337026	−0.185245	−0.116062	−0.075940
4	-	0.341393	0.492785	0.586692
6	-	-	0.936194	1.088348
8	-	-	-	1.501143

In a similar manner, we could obtain the synthesis filters. One can now easily check that

$$\Delta^n \widetilde{G}(z_1, z_2)|_{(0,0)} = 0 \quad \text{for } 0 \leq |n| < \widetilde{N} = 4 \quad \text{and}$$

$$\Delta^n G(z_1, z_2)|_{(0,0)} = 0 \quad \text{for } 0 \leq |n| < N = 2.$$

Fig. 6 shows the magnitudes of the Fourier transforms of the analysis and synthesis highpass filters while Fig. 7 shows the fifth iteration of the dual and primal wavelets, respectively.

To examine the regularity of the filters we obtained, we compute Sobolev regularity for the primal and dual lowpass filters with $\widetilde{N}$ and N vanishing moments, respectively. We look at the eigenvalues of the invariant transfer matrix $\mathbf{T}_r$, as explained in Section I-F. For our dilation matrix, both eigenvalues are $\sqrt{2}$; thus the special eigenvalues are powers of $\sqrt{2}$ and the Sobolev regularity is $s = \log_2 \rho$ with ρ the largest nonspecial eigenvalue. According to Theorem 2, if N and $\widetilde{N}$ are at least one and both transfer matrices have all eigenvalues inside the unit circle except for one $\lambda = 1$ (which is equivalent to both scaling functions having positive Sobolev regularity) then the biorthogonal

basis is stable. The results are given in Table III. All the primal scaling functions and all the duals with $N > 2$ have positive Sobolev smoothness. Note how the smoothness increases with both N and $\widetilde{N}$[1].

6) FCO Interpolating Filter Bank Families: The FCO or face centered orthorhombic lattice is the counterpart of the quincunx family in three dimensions. Thus $d = 3$ and $M = 2$, as in Fig. 8. One of the possible dilation matrices is given by

$$D = \begin{pmatrix} 1 & 0 & 1 \\ 1 & 1 & 0 \\ 0 & 1 & 1 \end{pmatrix}.$$

[1]After finishing this work, we learned that the $(2, 2)$ filter pair from this family was developed independently by Uytterhoeven. For more details we refer to [54].
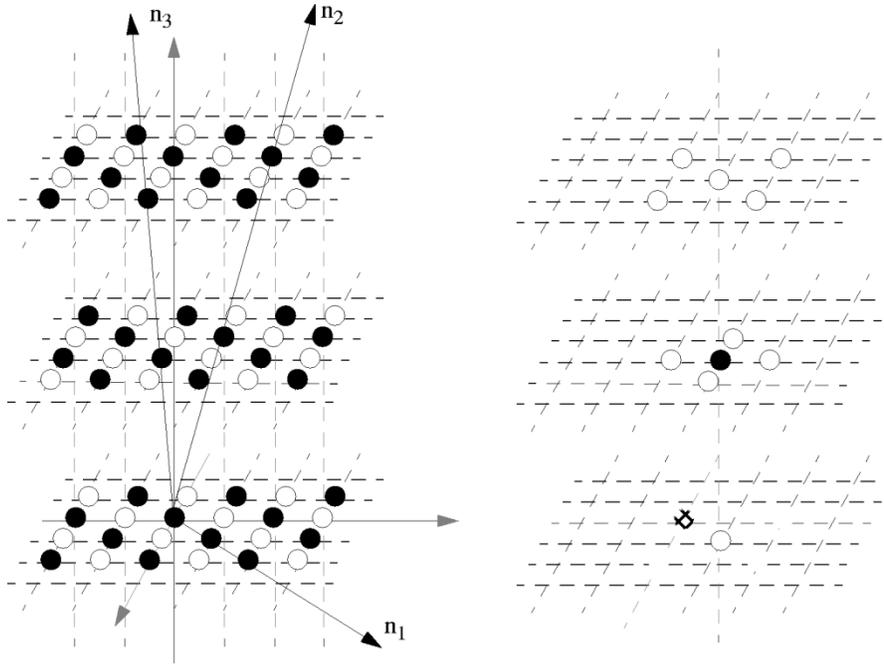
Fig. 8.   FCO lattice and the relevant neighborhood on the same lattice. The black point is the one to be interpolated, the white points constitute the first ring, while the checkered points constitute the second ring.

TABLE IV
FCO NEVILLE FILTERS. THE RINGS CORRESPOND TO RINGS GIVEN IN FIG. 8. THE NUMBERS IN PARENTHESES GIVE THE NUMBER OF POINTS IN EACH RING

		Numerator		Denominator
Taps	Order \ Ring	1(6)	2(8)	
6	2	1		6
14	4	4	-1	2^4

TABLE V
CHECKERBOARD NEVILLE FILTERS IN d DIMENSIONS

Taps	Order \ Ring	1(2d)	$2\left(8\binom{d}{3}\right)$
$2d$	2	$\frac{1}{2d}$	
$2d + 8\binom{d}{3}$	4	$\frac{3}{4d}$	$-\frac{1}{16\binom{d}{3}}$

The coset representative is $t_1 = (1,1,1)$. According to Theorem 9, the shift for the Neville filter is $\tau = D^{-1}t_1 = (1/2, 1/2, 1/2)$. Table IV gives Neville filters achieving linear and cubic interpolation. We will not explicitly construct filters here, as the process is the same as in the previous two sections. The only difference is that z^D in this setting is (z_1z_2, z_2z_3, z_1z_3). Note also that since D/D is not unitary, it is misleading to look for the neighborhoods in the sampled domain; instead, they are found on the original lattice.

7) General Checkerboard Lattices: The quincunx and FCO lattices are special cases of the so-called D_n or checkerboard lattice [11]. In the general d-dimensional case, a one-ring neighborhood contains $2d$ elements while the second ring contains $8\binom{d}{3}$ elements. The weights are given in Table V.

V. M-CHANNEL INTERPOLATING FILTER BANKS

In this section we consider the M-channel filter banks. Here $|D| = M$ and we have $M - 1$ cosets of the form $D\mathbf{Z}^d + t_j$ where $t_j \in \mathbf{Z}^d$. We have M polyphase components which we number with subscripts 0 to $M - 1$, thus

$$H(z) = \sum_{i=0}^{M-1} z^{-t_i} H_i(z^D).$$

Again we use two lifting steps for the ith channel ($1 \le i \le M - 1$), one predict (P_i) and one update (U_i) as in Fig. 9. Note that the ith predictor predicts the elements from the ith coset based on the elements from the 0th coset (original sampled lattice).

The polyphase matrix is now an $M \times M$ matrix given by

$$\mathcal{P} = \begin{bmatrix} 1 & U_1 & U_2 & \cdots & U_{M-1} \\ 0 & 1 & 0 & \cdots & 0 \\ 0 & 0 & 1 & \cdots & 0 \\ \vdots & \vdots & \vdots & \ddots & \vdots \\ 0 & 0 & 0 & \cdots & 1 \end{bmatrix}$$

$$\cdot \begin{bmatrix} 1 & 0 & 0 & \cdots & 0 \\ -P_1 & 1 & 0 & \cdots & 0 \\ -P_2 & 0 & 1 & \cdots & 0 \\ \vdots & \vdots & \vdots & \ddots & \vdots \\ -P_{M-1} & 0 & 0 & \cdots & 1 \end{bmatrix} \qquad (18)$$

$$= \begin{bmatrix} 1 - \sum_{i=1}^{M-1} U_iP_i & U_1 & U_2 & \cdots & U_{M-1} \\ -P_1 & 1 & 0 & \cdots & 0 \\ -P_2 & 0 & 1 & \cdots & 0 \\ \vdots & \vdots & \vdots & \ddots & \vdots \\ -P_{M-1} & 0 & 0 & \cdots & 1 \end{bmatrix} \qquad (19)$$
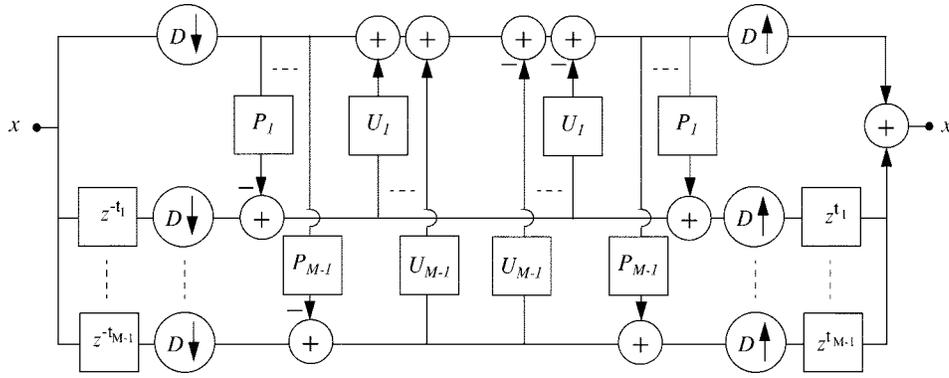
Fig. 9.   The M-channel lifting scheme. P_i and U_i stand for predict and update filters, respectively.

with adjoint inverse (see (20) and (21) shown at the bottom of this page). The condition for dual vanishing moments DM can now be found, similarly to the two-channel case, as

$$\widetilde{G}_j \pi(\mathbf{Z}^d) = \widetilde{G}_j^0 \pi(\mathbf{Z}^d) + \sum_{i=1}^{M-1} G_{j,i} \pi(\mathbf{Z}^d + t_i) = 0.$$

Substituting values from the jth row of the polyphase matrix $\mathcal{P}$ we get

$$P_j \pi(D\mathbf{Z}^d) = \pi(D\mathbf{Z}^d + t_j)$$
$$\text{for } \pi \in \Pi_{\widetilde{N}}, j = 1, \cdots, M - 1.$$

This implies that P_j is a Neville filter of order $\widetilde{N}$ with shift $\tau_j = D^{-1} t_j$. Similarly, the primal moments condition PM becomes

$$-U_j^* \pi(D\mathbf{Z}^d) - \sum_{i=1}^{M-1} U_j^* P_i^* \pi(D\mathbf{Z}^d + t_i)$$
$$+ \pi(D\mathbf{Z}^d + t_j) = 0, \quad \text{for } \pi \in \Pi_N,$$

for $j = 1, \cdots, M - 1$. Given that P_j is a Neville filter of order $\widetilde{N}$ with shift τ_j, if $N \le \widetilde{N}$ the above expression reduces to

$$M U_j^* \pi(D\mathbf{Z}^d) = \pi(D\mathbf{Z}^d + t_j), \quad \text{for } \pi \in \Pi_N.$$

Consequently, $M U_j^*$ is a Neville filter of order N with shift τ_j. We have thus just shown the following theorem:

Theorem 10: Let $N \le \widetilde{N}$. We can build a filter bank with N primal vanishing moments and $\widetilde{N}$ dual vanishing moments by letting the predict filters be Neville filters of order $\widetilde{N}$ with shifts $\tau_j = D^{-1} t_j$ and choosing the update filters as $1/M$ times the adjoints of Neville filters of order N with shifts $-\tau_j$.

Remarks:

1) The theorem results in Neville filters $P_j^{\widetilde{N}}$ with shifts $\tau_j = D^{-1} t_j$, and updates $U_j = P_j^{N*}/2$ which are not Neville filters per se, but are scaled versions of Neville filters P_j^{N*} with shifts $-\tau_j = -D^{-1} t_j$.

2) As before, if we need $N > \widetilde{N}$, we can always exchange the role of the primal and dual filters.

3) Not all of the predict filters have to be of the same order; each predict filter has to be at least of order $\widetilde{N}$. Similarly, each update filter has to have order at least N.

A. Examples of M-Channel Interpolating Filter Bank Families

1) One-Dimensional M-Channel Families: Coset representatives are here $t_i = i$ $(0 \le i < M)$ and the corresponding shifts are $\tau_i = i/M$. Thus P_i is a Neville filter with shift i/M. Given that $\tau_i = 1 - \tau_{M-i}$, we have that $P_i(z) = z P_{M-i}(1/z)$. Tables VI and VII give predict filters for the three- and four-channel cases.

2) Two-Dimensional Separable Families: An obvious extension to multiple dimensions is the tensor product of 1-D two-channel solutions. Then the dilation matrix is diagonal

$$D = \begin{pmatrix} 2 & 0 \\ 0 & 2 \end{pmatrix}.$$

The coset representatives from the unit cell are

$$t_0 = (0,0), \quad t_1 = (1,0), \quad t_2 = (0,1), \quad t_3 = (1,1)$$

$$\mathcal{P}^{*-1} = \begin{bmatrix} 1 & 0 & 0 & \cdots & 0 \\ -U_1^* & 1 & 0 & \cdots & 0 \\ -U_2^* & 0 & 1 & \cdots & 0 \\ \vdots & \vdots & \vdots & \ddots & \vdots \\ -U_{M-1}^* & 0 & 0 & \cdots & 1 \end{bmatrix} \begin{bmatrix} 1 & P_1^* & P_2^* & \cdots & P_{M-1}^* \\ 0 & 1 & 0 & \cdots & 0 \\ 0 & 0 & 1 & \cdots & 0 \\ \vdots & \vdots & \vdots & \ddots & \vdots \\ 0 & 0 & 0 & \cdots & 1 \end{bmatrix} \tag{20}$$

$$= \begin{bmatrix} 1 & P_1^* & P_2^* & \cdots & P_{M-1}^* \\ -U_1^* & 1 - U_1^* P_1^* & -U_1^* P_2^* & \cdots & -U_1^* P_{M-1}^* \\ -U_2^* & -U_2^* P_1^* & 1 - U_2^* P_2^* & \cdots & -U_2^* P_{M-1}^* \\ \vdots & \vdots & \vdots & \ddots & \vdots \\ -U_{M-1}^* & -U_{M-1}^* P_1^* & -U_{M-1}^* P_2^* & \cdots & 1 - U_{M-1}^* P_{M-1}^* \end{bmatrix} \tag{21}$$

TABLE VI
THREE-CHANNEL NEVILLE FILTERS. TABLE GIVES PREDICT FILTER P_1,
WHILE $P_2(z) = z\,P_1(1/z)$

	Numerator								Denominator
$N \setminus k$	3	2	1	0	-1	-2	-3	-4	
2				2	1				3
4			-5	60	30	-4			3^4
6		8	-70	560	280	-56	7		3^6
8	-44	440	-2310	15400	7700	-1848	385	-40	3^9

TABLE VII
FOUR-CHANNEL NEVILLE FILTERS. TABLE GIVES PREDICT FILTER P_1
WHILE P_2 CORRESPONDS TO THE DESLAURIERS-DUBUC PREDICT FILTER
AND $P_3(z) = z\,P_1(1/z)$

	Numerator								Denominator
$N \setminus k$	3	2	1	0	-1	-2	-3	-4	
2				3	1				2^2
4			-7	105	35	-5			2^7
6		77	-693	6930	2310	-495	63		2^{13}
8	-495	5005	-27027	225225	75075	-19305	4095	-429	2^{18}

with the corresponding shifts τ_i

$$\tau_1 = (1/2, 0), \quad \tau_2 = (0, 1/2), \quad \tau_3 = (1/2, 1/2).$$

Fig. 10 shows the original lattice as well as lattices in the sampled domain with interpolation neighborhoods. It is interesting to note that for the predict filters P_1 and P_3 neighborhoods turn out to be 1-D and thus P_1 and P_3 can be taken from Table I. Moreover, the neighborhoods for P_2 are the same as those in the quincunx case, and thus, P_2 can be taken from Table II.

3) Two-Dimensional Hexagonal Families: One of the possible sampling matrices in the hexagonal case is given by

$$D = \begin{pmatrix} 2 & 2 \\ 1 & -1 \end{pmatrix}.$$

Fig. 11 depicts the hexagonal lattice together with its unit cell and the coset representatives. The coset representatives are $t_i = (i, 0)$ for $i = 1, \cdots, 3$. According to Theorem 10, shifts for the Neville family we want to construct are $\tau_i = D^{-1}t_i = (i/4, i/4), i = 1, 2, 3$. We now have to find a way of predicting the t_1, t_2, t_3 points given the points on the hexagonal lattice. Fig. 11 gives neighborhoods for P_1; P_2 has the same neighborhoods as in the quincunx case and P_3 has the same neighborhoods as P_1 except time reversed in both dimensions. Table VIII gives weights for P_1 and interpolation orders $1, 2, 4, 6$ (P_2 is the same as in the quincunx case and $P_3(z) = z_1 P_1(1/z)$). We obtained these values as the output of the de Boor-Ron algorithm.

4) Triangular Edge Lattice: The triangular edge lattice and the downsampled lattice are shown in Fig. 12 (upper left). This is the first example where the original lattice is not $\mathbf{Z}^2$, rather it is $\mathcal{K} = \Gamma_{\text{triang}} \mathbf{Z}^2$ with Γ_{triang} from (4). It is called triangular edge, because new vertices live on edges. Structurally, this is the separable lattice of Section IV-A2, which can be seen by drawing the unit cell in an orthonormal coordinate system as in Fig. 12. Thus $D = 2I$ and $\tau_1 = (1/2, 0), \tau_2 = (0, 1/2), \tau_3 = (1/2, 1/2)$. However, the fact that the original lattice is organized in equilateral triangles leads to a different choice of neighborhoods which reflects the three symmetry axes of the lattice

as in Fig. 12. The neighborhoods for the three cosets are rotated copies of each other. Table IX gives the prediction filters of order $2, 4$, and 6. Note that the order 2 prediction will lead to piecewise linear scaling functions (pyramid functions), while the order 4 is the well-known Butterfly subdivision scheme [21]. The values for order 6 were obtained from the big Butterfly scheme [29].

5) Triangular Face Lattice: As opposed to the tridiagonal edge lattice, where the interpolation points are on the edges, the interpolation points in the triangular face lattice are in the middle of each triangle. A possible dilation matrix is given by

$$D = \begin{pmatrix} 2 & 1 \\ -1 & 1 \end{pmatrix}.$$

Fig. 13 depicts the triangular face lattice together with its unit cell and the coset representatives which are $t_i = (i, 0)$ with $i = 0, 1, 2$. According to Theorem 10, shifts for the Neville family we want to construct are $\tau_i = D^{-1}t_i = (i/3, i/3), i = 1, 2$. We now have to find a way of predicting the t_1, t_2 points given the points on the tridiagonal lattice. Fig. 13 gives neighborhoods for P_1. The neighborhoods for P_2 can be found on the same figure as well. Table X gives weights for P_1 and interpolation orders $2, 3$, and 5.

VI. FAST LIFTED WAVELET TRANSFORM

In this section, we discuss the implementation of the wavelet transform using lifting. Start with an input sequence $x = \{x_k | k \in \mathcal{K}\}$ and create M output sequences: one lowpass sequence $s = \{s_k | k \in \mathcal{K}\}$ and $M - 1$ highpass sequences $d_i = \{d_{i;k} | k \in \mathcal{K}, 1 \leq i \leq M\}$. Note that we can link each sample of the output sequences to a unique sample of the input sequence: s_k corresponds to x_{Dk} and $d_{i;k}$ corresponds to x_{Dk+t_i}. This correspondence combined with the lifting steps allows for in-place computation; instead of allocating new memory for the s and d_i sequences, we simply overwrite the corresponding elements in the x sequence. Lifting guarantees that we will never overwrite a sample we need later.

Denote the impulse response of the predict filter P_i to be $p_{i;k}$ and similarly for the update filters. The predict (and update) sequences are nonzero in a finite symmetric neighborhood around the origin $\mathcal{N}$: that is, $p_{i;k} \neq 0$ for $k \in \mathcal{N} \subset \mathcal{K}$. The transform can now be described by the following pseudocode:

```
Analysis
    for 1 ≤ i ≤ M - 1:
        for k ∈ 𝒦:
            x_{Dk+t_i} -= ∑_{l∈𝒩+𝒦} p_{i;k-l} x_{Dl}
    for 1 ≤ i ≤ M - 1:
        for k ∈ 𝒦:
            x_{Dk} += ∑_{l∈𝒩+𝒦} u_{i;k-l} x_{Dl+t_i}
```
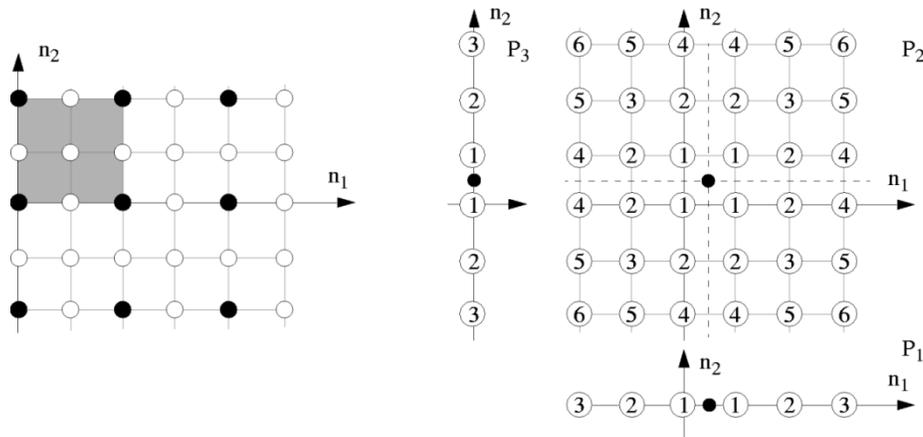
Fig. 10. Separable lattice with its unit cell and the lattices in the sampled domain with neighborhoods. The figure shows neighborhoods for predict filters P_1, P_2 and P_3.
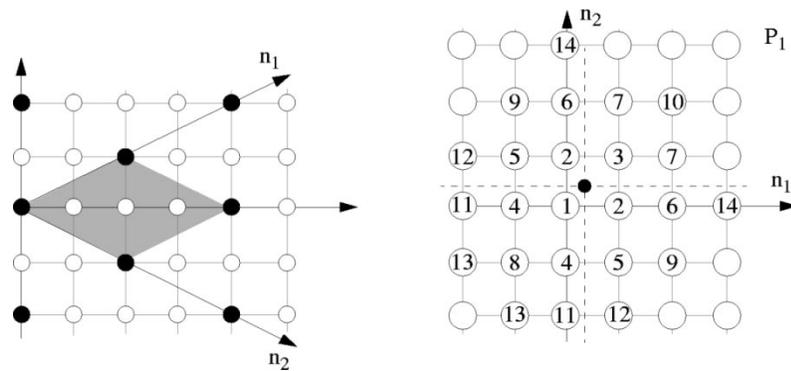
Fig. 11. Hexagonal lattice with its unit cell and the lattice in the sampled domain with neighborhoods. The figure gives only the neighborhood for P_1; P_2 is the same as in the quincunx case and P_3 has the same neighborhood as P_1 except time reversed in both dimensions. The small black dot within the first ring is the point $(1/4, 1/4)$ at which we want to interpolate.


```
Synthesis
    for 1 ≤ i ≤ M − 1:
        for k ∈ 𝒦:
            x_{Dk} − = ∑_{l∈𝒩+𝒦} u_{i;k−l} x_{Dl+t_i}
    for 1 ≤ i ≤ M − 1:
        for k ∈ 𝒦:
            x_{Dk+t_i} + = ∑_{l∈𝒩+𝒦} p_{i;k−l} x_{Dl}
```

The pseudocode illustrates one of the nice aspects of lifting: once the algorithm for the analysis is coded, the synthesis immediately follows by reversing the operations and flipping the signs. An integer-to-integer version can immediately be built by rounding off to the nearest integer before doing the $+ =$ or $- =$ operations [3].

To see how much lifting will speed up the computation, we look at the polyphase matrices in Section IV. Let us start with the analysis side. Equation (18) corresponds to the implementation using lifting, while (19) would correspond to a standard implementation. We try to get a cost estimate of each implementation. Assume that the cost of each predict and update filter is
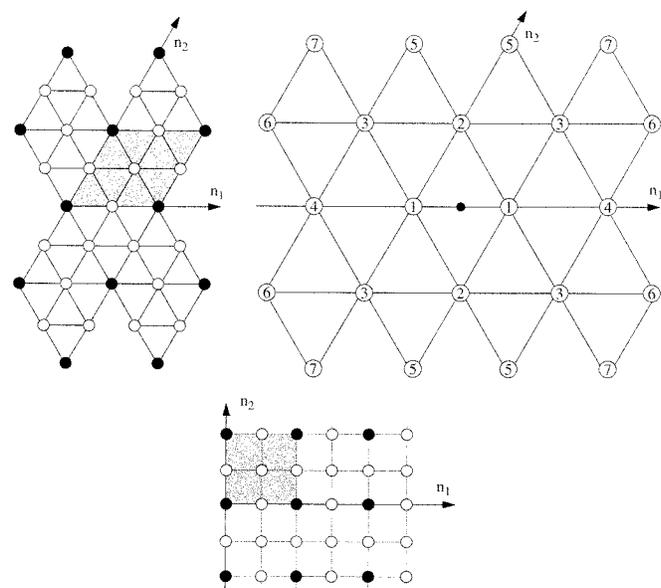
Fig. 12. Triangular edge lattice with its unit cell and the lattice in the sampled domain with neighborhoods. The small black dot within the first ring is the point $(1/2, 0)$ at which we want to interpolate. Observe that this lattice in the Cartesian coordinate system corresponds to the separable lattice.

the same and equal to C. Then, the cost of the lifting implementation is $2(M - 1)C$. The cost of the standard implementation
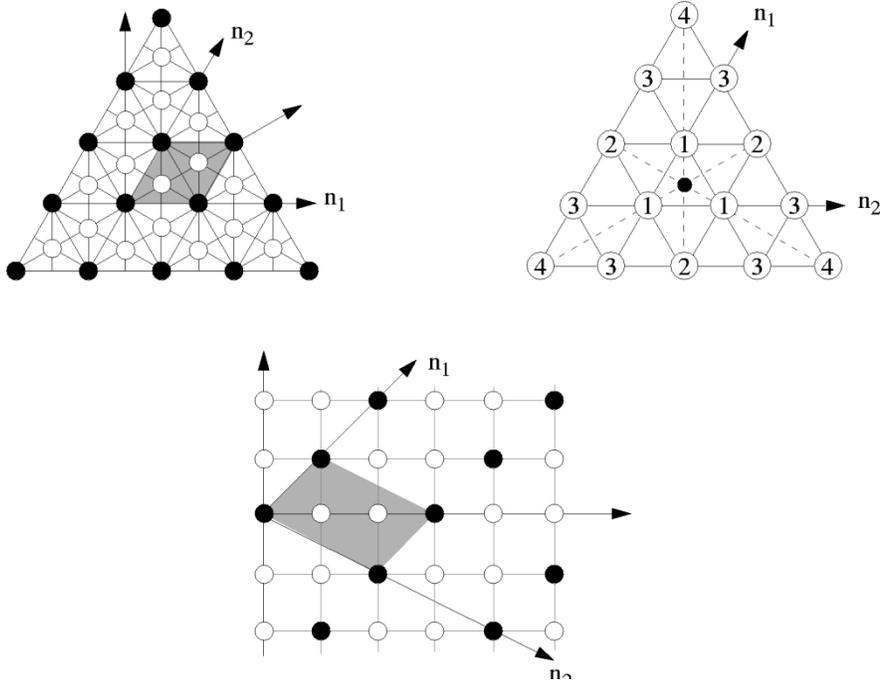
Fig. 13.   Triangular face lattice with its unit cell and the lattice in the sampled domain with the neighborhoods for P_1. The small black dot within the first ring is the point $(1/2, 0)$ at which we want to interpolate.

TABLE VIII

HEXAGONAL NEVILLE FILTERS. THE TABLE GIVES PREDICT FILTERS P_1; P_2 IS THE SAME AS IN THE QUINCUNX CASE AND $P_3(z) = z_1 P_1(1/z)$. (THE NUMBERS IN PARENTHESES GIVE THE NUMBER OF POINTS IN EACH RING. FOR SPACE REASONS, WE GIVE THE TRANSPOSED TABLE)

	Taps	4	12	18	24
	Order	2	4	5	6
Ring	Numer.				
1(1)		9	342	14385	46620
2(2)		3	114	2555	16590
3(1)		1	38	1225	3500
4(2)			−21	−1855	−5250
5(2)			−7	−245	−1260
6(2)			−15	−245	−3570
7(2)			−5	−175	−525
8(1)				49	1036
9(2)				35	35
10(1)				25	100
11(2)				280	546
12(2)					175
13(2)					−105
14(2)					504
	Denom.	2^4	2^9	2^{14}	2^{16}

TABLE IX

TRIANGULAR EDGE NEVILLE FILTERS. THE RINGS CORRESPOND TO RINGS GIVEN IN FIG. 12. THE NUMBERS IN PARENTHESES GIVE THE NUMBER OF POINTS IN EACH RING

Taps	Order \ Ring	Numerator							Denominator
		1(2)	2(2)	3(4)	4(2)	5(4)	6(4)	7(4)	
2	2	1							2^1
8	4	8	2	−1					2^4
22	6	558	102	−60	−46	−3	9	3	2^{10}

TABLE X

TRIANGULAR FACE NEVILLE FILTERS. THE RINGS CORRESPOND TO RINGS GIVEN IN FIG. 13. THE NUMBERS IN PARENTHESES GIVE THE NUMBER OF POINTS IN EACH RING

Taps	Order \ Ring	Numerator				Denominator
		1(3)	2(3)	3(6)	4(3)	
3	2	1				3^1
6	3	4	−1			3^2
15	5	96	12	−16	5	3^5

is the cost of lifting implementation plus the cost coming from the top left element in the polyphase matrix

$$1 - \sum_{i=1}^{M-1} U_i P_i.$$

If we use the above formula to implement this filter, the cost is $2(M-1)C$. The alternative is to expand the summation and then apply the expanded filter. Assuming that the neighborhoods of the predict and update filters are roughly balls in d dimensions, the cost of the expanded filter is $2^d C$. For low dimensions and high number of subbands this may be cheaper than $2(M-1)C$. In summary, on the analysis side the speed-up provided by lifting is roughly equal to

$$1 + \min\left(1, \frac{2^{d-1}}{M-1}\right).$$

If $2^{d-1} > M - 1$, that is, either high dimensions or low number of subbands, the speed-up is 2, otherwise it is lower. For low dimensions with high number of subbands the speed-up becomes insignificant. Separable lattices, where $M = 2^d$ form an intermediate case where the speed-up is roughly 1.5. With a similar analysis on the synthesis side using (20) and (21) we see that the synthesis speed-up becomes

$$\frac{2(M-1) + 2(M-1)^2}{2(M-1)} = M.$$

For $d = 1$ and $M = 2$ the speed-up on the analysis and synthesis side corresponds to the factor 2 from [15], [48]. For $M > 2$, the synthesis speed-up due to lifting is much higher than the analysis speed-up.

Remark:

One has to keep in mind that the speedup provided here is only relevant in case the filters are nonseparable. A separable filter can be implemented much faster as a succession of 1-D

filters in different dimensions. One can then use lifting as in [15] to speed up the 1-D filters. In general the Neville filters we computed are strictly nonseparable.

ACKNOWLEDGMENT

The authors thank P. Schröder for providing them with an implementation of the de Boor–Ron algorithm, J. Mazo for improving the exposition, and J. McDonald for pointing out a mistake in the FCO lattice construction in an earlier version.

REFERENCES

[1] R. Ansari, "Two-dimensional IIR filters for exact reconstruction in tree-structured subband decomposition," *Electron. Lett.*, vol. 23, pp. 633–634, June 1987.

[2] A. A. M. L. Bruckens and A. W. M. van den Enden, "New networks for perfect inversion and perfect reconstruction," *IEEE J. Select. Areas Commun.*, vol. 10, no. 1, 1992.

[3] R. Calderbank, I. Daubechies, and B.-L. Yeo, "Wavelet transforms that map integers to integers," *Appl. Comput. Harmon. Anal*, vol. 5, no. 3, pp. 332–369, 1998.

[4] T. Chen and P. P. Vaidyanathan, "Multidimensional multirate filters and filter banks derived from one-dimensional filters," *IEEE Trans. Signal Processing*, vol. 41, pp. 1749–1765, May 1993.

[5] C. K. Chui, ed., *Wavelets: A Tutorial in Theory and Applications*. San Diego, CA: Academic, 1992.

[6] C. K. Chui, J. Stöckler, and J. D. Ward, "Compactly supported box-spline wavelets," *Approx. Theory Applicat.*, vol. 8, no. 3, pp. 77–100, 1992.

[7] A. Cohen and I. Daubechies, "Non-separable bidimensional wavelet bases," *Rev. Mater. Iberoamer.*, vol. 9, no. 1, pp. 51–137, 1993.

[8] A. Cohen, I. Daubechies, and J. Feauveau, "Bi-orthogonal bases of compactly supported wavelets," *Commun. Pure Appl. Math.*, vol. 45, pp. 485–500, 1992.

[9] A. Cohen, K. Gröchenig, and L. Villemoes, "Regularity of multivariate refinable functions," preprint, 1996.

[10] A. Cohen and J.-M. Schlenker, "Compactly supported bidimensional wavelet bases with hexagonal symmetry," *Constr. Approx.*, vol. 9, no. 2, pp. 209–236, 1993.

[11] J. H. Conway and N. J. A. Sloane, *Sphere Packings, Lattices and Groups*. Berlin, Germany: Springer-Verlag, 1992.

[12] W. Dahmen, "Stability of multiscale transformations," *J. Fourier Anal. Applicat.*, vol. 2, no. 4, pp. 341–361, 1996.

[13] I. Daubechies, "Orthonormal bases of compactly supported wavelets," *Commun. Pure Appl. Math.*, vol. 41, pp. 909–996, 1988.

[14] ——, *Ten Lectures on Wavelets. CBMS-NSF Regional Conf. Series in Appl. Math.*. Philadelphia, PA: Soc. Ind. Appl. Math., 1992, vol. 61.

[15] I. Daubechies and W. Sweldens, "Factoring wavelet transforms into lifting steps," *J. Fourier Anal. Applicat.*, vol. 4, no. 3, pp. 247–269, 1998.

[16] C. de Boor, R. A. DeVore, and A. Ron, "On the construction of multivariate pre-wavelets," *Constr. Approx.*, vol. 9, no. 2, pp. 123–166, 1993.

[17] C. de Boor and A. Ron, "On multivariate polynomial interpolation," *Constr. Approx.*, vol. 6, pp. 287–302, 1990.

[18] ——, "Computational aspects of polynomial interpolation in several variables," *Math. Comput.*, vol. 58, pp. 705–727, 1992.

[19] G. Deslauriers and S. Dubuc, "Interpolation dyadique," in *Fractals, Dimensions Non Entières et Applications*, Masson, Paris, 1987, pp. 44–55.

[20] D. E. Dudgeon and R. M. Mersereau, *Multidimensional Digital Signal Processing*. Englewood Cliffs, NJ: Prentice-Hall, 1984.

[21] N. Dyn, D. Levin, and J. Gregory, "A butterfly subdivision scheme for surface interpolation with tension control," *ACM Trans. Graph.*, vol. 9, no. 2, pp. 160–169, 1990.

[22] R. A. Gopinath and C. S. Burrus, "On the moments of the scaling function," in *Proc. IEEE ISCAS,*, 1992, pp. 963–966.

[23] A. Grossmann and J. Morlet, "Decomposition of Hardy functions into square integrable wavelets of constant shape," *SIAM J. Math. Anal.*, vol. 15, no. 4, pp. 723–736, 1984.

[24] R.-Q. Ja, "Approximation properties of multivariate wavelets," *Math. Comput.*, to be published.

[25] ——, "Characterization of smoothness of multivariate refinable functions in Sobolev spaces," *Trans. Amer. Math. Soc.*, to be published.

[26] A. C. M. Kalker and L. A. Shah, "A group theoretic approach to multidimensional filter banks: Theory and applications," *IEEE Trans. Signal Processing*, vol. 44, pp. 1392–1405, June 1996.

[27] G. Karlsson and M. Vetterli, "Theory of two-dimensional multirate filter banks," *IEEE Trans. Acoust., Speech, Signal Processing*, vol. 38, pp. 925–937, June 1990.

[28] J. Kovačević and M. Vetterli, "Nonseparable multidimensional perfect reconstruction filter banks and wavelet bases for $\mathbf{R}^n$," *IEEE Trans. Inform. Theory*, vol. 38, pp. 533–555, Feb. 1992.

[29] O. Labkovsky, "The extended butterfly interpolatory scheme for the generation of c^2 surfaces," M.S. thesis, School Math. Sci., Tel-Aviv University, Tel-Aviv, Israel, 1996.

[30] S. G. Mallat, "Multiresolution approximations and wavelet orthonormal bases of $L^2(\mathbf{R})$," *Trans. Amer. Math. Soc.*, vol. 315, no. 1, pp. 69–87, 1989.

[31] T. G. Marshall, "U-L block-triangular matrix and ladder realizations of subband codes," in *Proc. IEEE Int. Cconf. Acoustics, Speech, Signal Prpcessing*, vol. 3, 1993, pp. 177–180.

[32] J. McClellan, "The design of two-dimensional filters by transformations," in *7th Annu. Princeton Conf. ISS*, Princeton, NJ, 1973, pp. 247–251.

[33] Y. Meyer, *Ondelettes et Opérateurs, I: Ondellettes, II: Opérateurs de Calderón-Zygmund, III: (with R. Coifman), Opérateurs Multilinéaires*. Hermann, France: Cambridge Univ. Press, English translation of vol. 1, 1993.

[34] F. Mintzer, "Filters for distortion-free two-band multirate filter banks," *IEEE Trans. Acoust., Speech, Signal Processing*, vol. ASSP-33, pp. 626–630, 1985.

[35] L.-M. Riessell, "Wavelet multiresolution representation of curves and surfaces," *CVGIP: Graph. Models Image Process.*, vol. 58, no. 2, pp. 198–217, 1996.

[36] S. D. Riemenschneider and Z. Shen, "Wavelets and pre-wavelets in low dimensions," *J. Approx. Theory*, vol. 71, no. 1, pp. 18–38, 1992.

[37] ——, "Construction of compactly supported biorthogonal wavelets in $l_2(r^s)$", preprint, Univ. Alberta, Edmonton, Alta, Canada, 1997.

[38] ——, "Multidimensional interpolatory subdivision schemes," *SIAM J. Numer. Anal.*, vol. 34, no. 6, pp. 2357–2381, 1997.

[39] S. D. Riemenschneider and Z. Shen, *Approximation Theory and Functional Analysis*, New York: Academic, 1991.

[40] A. Ron and Z. Shen, "Sobolev regularity of refinable functions," preprint, 1997.

[41] G. Schuller, "A new factorization and structure for cosine modulated filter banks with variable system delay," in *Proc. Asilomar Conf. Signals, Systems, Computers*, Pacific Grove, CA, 1996.

[42] G. D. T. Schuller and M. J. T. Smith, "New framework for modulated perfect reconstruction filter banks," *IEEE Trans. Signal Processing*, vol. 44, pp. 1941–1954, Aug. 1996.

[43] I. Shah and T. A. C. M. Kalker, "On ladder structures and linear phase conditions for bi-orthogonal filter banks," in *Proc. ICASSP '94*, 1994, pp. 181–184.

[44] M. J. T. Smith and T. P. Barnwell, "Exact reconstruction techniques for tree-structured subband codes," *IEEE Trans. Acoust., Speech, Signal Processing*, vol. ASSP-34, no. 3, pp. 434–441, 1986.

[45] J. Stöckler, "Multivariate wavelets," in *Wavelets: A Tutorial in Theory and Applications*. San Diego, CA: Academic, 1992, pp. 325–326.

[46] J. Stoer and R. Bulirsch, *Introduction to Numerical Analysis*, New York: Springer-Verlag, 1980.

[47] G. Strang and T. Nguyen, *Wavelets and Filter Banks*. Cambridge, MA: Wellesley, 1996.

[48] W. Sweldens, "The lifting scheme: A custom-design construction of biorthogonal wavelets," *Appl. Comput. Harmon. Anal.*, vol. 3, no. 2, pp. 186–200, 1996.

[49] ——, "The lifting scheme: A construction of second generation wavelets," *SIAM J. Math. Anal.*, vol. 29, no. 2, pp. 511–546, 1997.

[50] W. Sweldens and R. Piessens, "Quadrature formulae and asymptotic error expansions for wavelet approximations of smooth functions," *SIAM J. Numer. Anal.*, vol. 31, no. 4, pp. 1240–1264, 1994.

[51] D. B. H. Tay and N. G. Kingsbury, "Flexible design of multidimensional perfect reconstruction FIR 2-band filters using transformations of variables," *IEEE Trans. Image Processing*, vol. 2, pp. 466–480, Oct. 1993.

[52] J. Tian and R. O. Wells, "Vanishing moments and biorthogonal wavelet systems," in *Mathematics in Signal Processing IV*. Oxford, U.K.: Oxford Univ. Press, 1996.

[53] L. M. G. Tolhuizen, H. D. L. Hollimann, and T. A. C. M. Kalker, "On the realizability of bi-orthogonal M-dimensional 2-band filter banks," *IEEE Trans. Signal Processing*, vol. 43, pp. 640–648, Mar. 1995.

[54] G. Uytterhoeven and A. Bultheel, "The Red-Black wavelet transform," Dept. Comput. Science, Katholieke Universiteit, Leuven, Belgium, TW Rep. 271, Dec. 1997.

[55] P. P. Vaidyanathan, "Theory and design of M-channel maximally decimated quadrature mirror filters with arbitrary M, having perfect reconstruction property," *IEEE Trans. Acoust., Speech, Signal Processing*, vol. ASSP-35, no. 2, pp. 476–492, 1987.

[56] ——, *Multirate Systems and Filter Banks*. Englewood Cliffs, NJ: Prentice-Hall, 1992.

[57] M. Vetterli, "Filter banks allowing perfect reconstruction," *Signal Process.*, vol. 10, pp. 219–244, 1986.

[58] M. Vetterli and C. Herley, "Wavelets and filter banks: Theory and design," *IEEE Trans. Acoust., Speech, Signal Processing*, vol. ASSP-40, no. 9, pp. 2207–2232, 1992.

[59] M. Vetterli and J. Kovačević, *Wavelets and Subband Coding*. Englewood Cliffs, NJ: Prentice-Hall, 1995.

Wim Sweldens (M'97) received the Ph.D. degree in 1994 from the Katholieke Universiteit Leuven, Leuven, Belgium.

He was then with the University of South Carolina and Interval Research. He is now Member of Technical Staff at the Mathematics Center, Bell Laboratories, Lucent Technologies, Murray Hill, NJ. He introduced "lifting" as a technique to generalize wavelet transforms to complex geometries. His current research concerns the design of multiresolution and overcomplete representations and their applications in computer graphics, signal processing, and multiple antenna communications. He is the founding editor of the *Wavelet Digest*.

Jelena Kovačević (S'88–M'91–SM'96) received the Dipl.Elect.Eng. degree from the Electrical Engineering Department, University of Belgrade, Belgrade, Yugoslavia, in 1986, and the M.S. and Ph.D. degrees from Columbia University, New York, NY, in 1988 and 1991, respectively.

In November 1991, she joined AT&T Bell Laboratories (now Lucent Technologies), Murray Hill, NJ, as Member of Technical Staff. In the Fall of 1986, she was a Teaching Assistant at the University of Belgrade. From 1987 to 1991, she was a Graduate Research Assistant at Columbia University. In the Summer of 1985, she was with Gaz de France, Paris, France. During the Summer of 1987, she was with INTELSAT, Washington, DC, and in the Summer of 1998, with Pacific Bell, San Ramon, CA. Her research interests include wavelets, multirate signal processing, data compression, and signal processing for communications. She is a coauthor of the book (with M. Vetterli) *Wavelets and Subband Coding* (Englewood Cliffs, NJ: Prentice-Hall, 1995). She is on the editorial boards of the *Journal of Applied and Computational Harmonic Analysis*, *Journal of Fourier Analysis and Applications*, and *Signal Procesing Magazine*.

Dr. Kovačević received the Belgrade October Prize, the highest Belgrade prize for student scientific achievements awarded for the Engineering Diploma Thesis in October 1986, and the E. I. Jury Award at Columbia University for outstanding achievement as a graduate student in the areas of systems, communication, or signal processing. She served as an Associate Editor of the IEEE TRANSACTIONS ON SIGNAL PROCESSING and as a Guest Co-Editor (with I. Daubechies) of the Special Issue on Wavelets of the PROCEEDINGS OF THE IEEE. She is on the IMDSP Technical Committee of the IEEE Signal Processing Society and was a General Co-Chair (with J. Allebach) of the *9th Workshop on Image and Multidimensional Signal Processing*.